



HAL
open science

Thresholds in Origin of Life Scenarios

Cyrille Jeancolas, Christophe Malaterre, Philippe Nghe

► **To cite this version:**

Cyrille Jeancolas, Christophe Malaterre, Philippe Nghe. Thresholds in Origin of Life Scenarios. *iScience*, 2020, 23, pp.101756 -. 10.1016/j.isci.2020.101756 . hal-03493116

HAL Id: hal-03493116

<https://hal.science/hal-03493116v1>

Submitted on 21 Nov 2022

HAL is a multi-disciplinary open access archive for the deposit and dissemination of scientific research documents, whether they are published or not. The documents may come from teaching and research institutions in France or abroad, or from public or private research centers.

L'archive ouverte pluridisciplinaire **HAL**, est destinée au dépôt et à la diffusion de documents scientifiques de niveau recherche, publiés ou non, émanant des établissements d'enseignement et de recherche français ou étrangers, des laboratoires publics ou privés.



Distributed under a Creative Commons Attribution - NonCommercial 4.0 International License

1 **Thresholds in origin of life scenarios**

2 **Cyrille Jeancolas^{1,2}, Christophe Malaterre³, Philippe Nghe^{1*}**

3 ¹, Laboratoire de Biochimie, CBI, ESPCI Paris, Université PSL, CNRS, 75005 Paris, France

4 ², Laboratoire d'Anthropologie Sociale, Collège de France, 52 rue du Cardinal Lemoine,
5 75005 Paris, France

6 ³, Département de philosophie and Centre de recherche interuniversitaire sur la science et la
7 technologie (CIRST), Université du Québec à Montréal, 455, Boulevard René-Lévesque Est
8 Montréal (Québec) H3C 3P8, Canada

9

10 **Summary**

11 Thresholds are widespread in origin of life scenarios, from the emergence of chirality, to the
12 appearance of vesicles, of autocatalysis, all the way up to Darwinian evolution. Here, we analyze the
13 “error threshold” — which poses a condition for sustaining polymer replication — and generalize the
14 threshold approach to other properties of prebiotic systems. Thresholds provide theoretical
15 predictions, prescribe experimental tests and integrate interdisciplinary knowledge. The coupling
16 between systems and their environment determines how thresholds can be crossed, leading to
17 different categories of prebiotic transitions. Articulating multiple thresholds reveals evolutionary
18 properties in prebiotic scenarios. Overall, thresholds indicate how to assess, revise and compare origin
19 of life scenarios.

20

21 **Keywords:** thresholds, abiogenesis, origin of life, major transitions, prebiotic systems, evolution

22

23 **Introduction**

24 The transition from non-living to living matter is usually formulated in a historical manner, aiming to
25 address the origin of life on Earth (Oparin, 1938; de Duve, 1991). However, the sparsity of historical
26 evidence suggests that the “origin of life cannot be discovered; it has to be reinvented” (Eschenmoser
27 and Loewenthal, 1991). This view, together with increasing experimental possibilities and the
28 question of life on exoplanets (Rimmer *et al.*, 2018) broadens the field of investigation to synthetic
29 systems with lifelike properties (Solé, 2016), such as metabolism, reproduction and evolution
30 (Attwater and Holliger, 2014).

* Correspondence:
philippe.nghe@espci.psl.eu (P.N.), Lead Contact
cyrille.jeancolas@espci.psl.eu (C.J)
malaterre.christophe@uqam.ca (C.M.)

31 Origin of life scenarios consist of successions of transitions. Major transitions have been outlined
32 (Smith and Szathmáry, 1995; Szathmáry, 2015) but there are so far few empirical validations. Indeed,
33 experiments may face huge parameter spaces and waiting times. Furthermore, studying transitions
34 requires inputs from many disciplines, including chemistry, biochemistry, molecular biology,
35 evolutionary biology, physics, astrophysics, geology, or geochemistry among others (Preiner *et al.*,
36 2019). Thus, it remains a challenge to decompose scenarios at a sufficiently fine-grained scale for
37 experimental tests to be possible, while allowing articulation of elementary steps and overall
38 plausibility estimates.

39 Here, we propose thresholds to be an operational notion that can be used to decompose origin of life
40 scenarios, articulate theory and experiment, and assess scenario plausibility by coordinating
41 interdisciplinary efforts. A threshold can be defined as a major qualitative change undergone by a
42 physical-chemical system upon relatively minor changes in the values of systemic or environmental
43 control parameters. One of the most studied thresholds is Eigen's "error threshold" which constrains
44 replication-based scenarios of early genetic polymers (Eigen, 1971; Kun *et al.*, 2015; Takeuchi,
45 Hogeweg and Kaneko, 2017). A number of other prebiotic transitions invoke thresholds explicitly or
46 implicitly: the appearance of homochirality (Hawbaker and Blackmond, 2019), replication
47 (Kauffman, 1986; Szathmáry, 2006), compartmentalization (Hargreaves, Mulvihill and Deamer,
48 1977), Darwinian evolution (Goldenfeld, Biancalani and Jafarpour, 2017).

49 Below, we first sample the diversity of thresholds found in origin of life research. Thresholds are
50 encountered at different stages and levels of organization. In the second section, as a case study, we
51 examine the original formulation of the "error threshold" for template-based replication, highlighting
52 its interdisciplinary nature. In the third section, we analyze revisions to the error threshold that aim at
53 establishing more precise or more plausible models. In the fourth section, we generalize the threshold
54 approach to properties of prebiotic systems other than replication. Introducing a phase diagram
55 representation allows us to categorize different types of threshold transitions as a function of the
56 relationship between systems and their environment. In the fifth section, we investigate how to
57 articulate multiple thresholds toward building complete scenarios. In turn, we determine qualitative
58 relationships between transitions, such as entrenchment, contingency or transience. These
59 relationships are typically used in evolutionary biology but are more generally applicable to prebiotic
60 threshold transitions. Finally, we discuss how thresholds can be used to coordinate research efforts to
61 study the origin of life.

62

63 1. The diversity of thresholds in origin of life

64 In this section, we illustrate the diversity of threshold-type transitions in origin of life research with a
65 non-exhaustive list of examples taken from chemistry and thermodynamics all the way up to
66 evolutionary and Darwinian dynamics.

67 The prebiotic synthesis of the building blocks of life (i.e. amino acids, nucleic acids, sugars, fatty
68 acids) requires reactants to reach sufficient concentrations for the reactions to take place, hence the
69 existence of concentration thresholds. Concentration thresholds can be overcome by acting on
70 physical-chemical conditions resulting from enclosure into vesicles (Luisi, Stano and de Souza, 2014),
71 wet-dry cycles (Nelson *et al.*, 2001), freeze-thaw cycles (Monnard, Kanavarioti and Deamer, 2003;
72 Trinks, Schröder and Biebricher, 2005), adsorption on mineral surfaces (Lambert, 2008) or

73 thermophoresis effects in hydrothermal vents (Baaske *et al.*, 2007). Eutectic ice and meteoritic
74 impacts have been pointed out to overcome a concentration threshold of hydrogen cyanide for its
75 polymerization into purines (Miyakawa, Cleaves and Miller, 2002; Parkos *et al.*, 2018) (figure 1.a).
76 This pathway to purines includes yet another threshold which concerns free-energy barriers for the
77 formation of intermediate compounds, which could be overcome through exposition to light
78 (Boulanger *et al.*, 2013) (figure 1.b). Since the famous Miller’s experiment (Miller, 1953), lightning is
79 often considered to overcome such energy thresholds as well. The subsequent polymerization of
80 building blocks (e.g. nucleotides) must also overcome energy thresholds (Dickson, Burns and
81 Richardson, 2000), through chemical activation (Wachowius and Holliger, 2019) or adsorption on
82 mineral surfaces (Hazen and Sverjensky, 2010). More generally, when it comes to forming the
83 chemical bonds of biomolecules, a kinetic barrier has been estimated to be around 100 kJ/mol at
84 moderate temperature (Pascal, 2012). Another threshold transition in prebiotic chemistry concerns the
85 emergence of homochirality among biomolecules, i.e. the fact that in extant life amino acids are left-
86 handed and sugars right-handed (Hawbaker and Blackmond, 2019).

87 The emergence of prebiotic compartments can be studied as a phase transition in the thermodynamic
88 sense. Several thresholds that separate phases of dissociated components from self-assembled
89 structures have been identified. Self-assembly thresholds controlling compartments formation can be
90 overcome by varying physical-chemical parameters such as pH, temperature, or molecular crowding.
91 It has been studied for the formation of vesicles (Bachmann, Luigi and Lang, 1992), coacervates
92 (Jiang *et al.*, 2015) or microdomains in liquid crystals (Todisco *et al.*, 2018) (figure 1.c). For finite-
93 size structures, such as peptide nanospheres (Carny and Gazit, 2005), mathematical models have
94 established a threshold separating the self-assembled state from a “yield catastrophe phase” where
95 constituents nucleate without stabilizing to final structures, controlled by activation and dimerization
96 rates (Gartner *et al.*, 2020).

97 Transitions toward self-organization in reaction networks require the spontaneous formation of
98 autocatalytic networks (Kauffman, 1993) (figure 1.d). A first threshold concerns catalytic closure,
99 initially formulated for a model of networks of ligation and fragmentation reactions between peptides
100 (Kauffman, 1986). Catalytic closure implies the existence of a set of peptides such that the formation
101 of any member of the set is catalyzed by another member of the set. In this model, the transition
102 happens when $\frac{E}{N} > \frac{1}{2}$, with E being the number of catalyzed reactions and N the number of peptides
103 (respectively edges and nodes of the network) (Cohen, 1988). Other models have simulated
104 autocatalytic transitions in the context of template-based replication (Chen and Nowak, 2012; Mathis,
105 Bhattacharya and Walker, 2017). Wu *et al.* for instance examined how variations in catalytic feedback
106 efficiency and spontaneous polymerization rate could induce the crossing of a threshold delimiting a
107 regime of slow spontaneous RNA synthesis from a regime of rapid autocatalytic RNA synthesis
108 (figure 1.e). This transition is stochastic, meaning that the systems explore random chemical
109 compositions in a fixed environment before undergoing the transition.

110 Once formed, autocatalytic networks need to be sustained. For this, catalysts within autocatalytic
111 networks should exhibit high enough specificity towards the reactions of the network to overcome
112 degradation and losses due to side reactions. Given an autocatalytic set of p reactions, each catalyzed
113 with a specificity s_i (where $i = 0, \dots, p$), disappearance can be avoided provided $\prod_{i=1 \dots p} s_i > \frac{1}{2}$,
114 thereupon revealing a “decay threshold” (Szathmáry, 2006; Vasas *et al.*, 2012; Blokhuis, Lacoste and
115 Nghe, 2020). Furthermore, for survival to be possible, the concentration of feedstock compounds must
116 stay above a specific value most of the time. For a single autocatalytic reaction, this condition is

117 fulfilled if $R > \frac{a}{k}$, with R being the concentration of reactants, a the degradation kinetic coefficient of
118 the autocatalyst and k the kinetic rate of autocatalyst production (King, 1977).
119

120 Later stages in origin of life concern the emergence of template-based replication of genetic polymers,
121 which is discussed in detail in the next section, and the emergence of protocells. Early compartments
122 and genetic polymers may not have been strictly associated in lineages. Indeed, compartments provide
123 a way for multilevel selection (Poole, 2009) even when genes are submitted to pooling and mixing
124 (Matsumura *et al.*, 2016). The “progenote stage” has been described as a stage where genes heavily
125 exchange between dividing protocells via horizontal gene transfer (HGT) (Woese and Fox, 1977). The
126 transition from dominant HGT to lineages where genetic polymers and compartments are strongly
127 correlated has been coined the “Darwinian threshold” (Woese, 2002) (figure 1.f). Mathematical
128 models (Arnoldt, Strogatz and Timme, 2015; Goldenfeld, Biancalani and Jafarpour, 2017) show that
129 such a threshold can be crossed when the progenotes HGT rate decreases below a specific value. This
130 decrease might result from mutations and environmental changes such as protocell density, alkaline
131 shifts, or nutrient limitation (Claverys, Prudhomme and Martin, 2006; Kovács *et al.*, 2009). In
132 contrast, other authors posit the advent of Darwinian evolution before the appearance of protocells.
133 This is the case of Eigen’s theory of template-based replication of genetic polymers (Eigen, 1971;
134 Eigen and Schuster, 1977; Eigen, McCaskill and Schuster, 1988), which we detail in the coming
135 section.

136

137 2. The error threshold and the replicase

138 The error-threshold, introduced by Eigen (1971), has certainly been the most studied threshold in
139 origin of life theories. We draw here on the main findings to make a case study and highlight the
140 usefulness of studying thresholds, the replicase scenario being reviewed elsewhere (Kun *et al.*, 2015;
141 Takeuchi, Hogeweg and Kaneko, 2017). In the RNA world hypothesis, an RNA capable of catalyzing
142 the polymerization of its own sequence as well as others (Cheng and Unrau, 2010), a generalist *self-*
143 *replicase*, is regarded as a primordial replicator capable of Darwinian evolution. The appearance and
144 maintenance of such a replicase regime—a process that we will refer to as the “replicase scenario”—
145 is constrained by the error threshold which imposes upper bounds on the length of the copied
146 reference sequences given an error-rate during replication. More specifically, to avoid the
147 disappearance of the sequence to be copied across rounds of replication, called the “error
148 catastrophe”, the following condition must be fulfilled:

$$l \leq \frac{\ln(s)}{e} \quad (1)$$

149 where e is the replicase copying error rate and s the selective advantage, defined as the ratio of the
150 replication rate of the reference sequence to that of the erroneous sequences. Note that formula (1)
151 was initially derived by Eigen *et al.* assuming that a polymerase is present and non-limiting or that
152 replication is non-enzymatic (see next section for more precise models). Formula (1) is valid for $s >$
153 1, otherwise this model forbids any reference sequence, including the replicase, to be sustainable.

154 From (1), we deduce a function $e_{max} = \frac{\ln(s)}{l}$ (red curve on figure 2.a). Due to the minimum structure
155 complexity required for replicase activity, replicases of a given length l cannot reach perfect fidelity
156 and their error rate must be above a certain value $e_{min}(l)$ (blue curve on figure 2.a). Bounds e_{min}

157 and e_{max} delineate a domain in the space parametrized by (l, e) so that above e_{min} there exist
 158 replicases, and under e_{max} , replicase copying can be sustained through faithful replication. If these
 159 domains overlap, i.e. if there exists an l such that $e_{max}(l) \geq e_{min}(l)$, then the replicase regime is
 160 possible in the intersection domain (green zone in figures 2.a and 2.b; note that the sheer possibility of
 161 the replicase regime does not imply its plausibility). Otherwise, $e_{max}(l) < e_{min}(l)$ for all l , and the
 162 replicase regime has no existence domain (figure 2.c). The latter case corresponds to the so-called
 163 ‘‘Eigen’s paradox’’: no long replicases without replication fidelity, but no fidelity without long
 164 replicases.

165 If the replicase regime is possible, the next step is to study the plausibility of emergence of a
 166 sustainable replicase. First needed is the number N_l of sequences of length l that have a replicase
 167 activity with an error rate e . The higher this number, the greater the chances of reaching at least one
 168 such replicase by a pre-existing generative process. The distribution $f(e, l)$ of these sequences is
 169 depicted in figure 2.d for a given length l . Second, the pre-existing generative process also determines
 170 the plausibility of the transition. A typical model for this regime is random polymerization, where
 171 every sequence is generated with equal probability for a given length. There, the fraction of generated
 172 polymers of a certain length $g(l)$ in the polymer population decreases rapidly with l . From the
 173 distributions $f(e, l)$ and $g(l)$, we estimate the probability for a sustainable replicase to appear to be:

$$P_r = \sum_l g(l) \int_{e_{min}(l)}^{e_{max}(l)} f(e, l) de \quad (2)$$

174 This probability can be used in the context of an environmental scenario supplying estimates of the
 175 total number N of random oligomers present at any moment, their global renewal rate ρ resulting
 176 from sequence generation and destruction dynamics. The typical time t required for one replicase to
 177 appear then obeys:

$$\rho t N P_r \sim 1 \quad (3)$$

178 The parameters found in (2) and (3) highlight the highly interdisciplinary nature of the question: the
 179 threshold e_{max} is determined by replication dynamics studied in theoretical biology; the distribution f
 180 and threshold e_{min} arise from genotype-to-function relationships obtained from biochemical
 181 considerations; g depends on the chemistry of spontaneous polymerization; ρ and N depend on
 182 geochemical processes, and t should be compared with estimates from geology and planetary system
 183 stability analysis.

184 The analysis leading to (3) is only part of the answer for the replicase scenario: for the replication
 185 dynamics to actually start, a replicase needs to encounter either a copy of its own sequence or a
 186 complementary sequence. This should probably take place in a compartmentalized setting, where only
 187 replicase sequences are present, since otherwise the copying of other sequences would immediately
 188 take over the population. Furthermore, the analysis presented so far may be questioned, given that
 189 formula (1-3) rely on a number of strong assumptions. We examine some of these considerations in
 190 the coming section.

191

192 3. Refining and revising the replicase scenario

193 The error threshold of equation (1) relies on a number of simplifying assumptions that have been
194 refined in subsequent models presented here. Such models may lead to lower e_{max} , thus reducing the
195 size of the green zone in figure 3, which goes to the detriment of the replicase scenario. For instance,
196 Eigen’s original model ignores the effects of changes in replicase concentration, whereas the latter is
197 impacted by replication. Including this aspect greatly lowers e_{max} (Obermayer and Frey, 2009).
198 Experimental data about RNA replication highlight another required model revision, because
199 replication errors typically lead to shorter sequences rather than to point mutations (Ichihashi and
200 Yomo, 2016). As a result, mutants tend to replicate faster than the original sequence, which means
201 $s < 1$ by definition of the selective advantage, so that replicase regimes cannot be sustained (see
202 Section 2). Note however that it is still unclear whether results obtained with protein replicases used
203 in these experiments extrapolate to hypothetical RNA replicases. In contrast, other model refinements
204 tend to increase e_{max} , thus broadening the range of viable replicases. This is the case when
205 considering the abundance of neutral mutations in the neighborhood of the replicase sequence, leading
206 to a “relaxed” error threshold which is significantly lower than Eigen’s (Kun, Santos and Szathmary,
207 2005; Takeuchi, Poorthuis and Hogeweg, 2005).

208 Other modifications are revisions of the scenario. So-called “hypercycles” were first proposed as a
209 way to increase the robustness of the system to replication errors (Eigen and Schuster, 1977). This
210 model is based on a network with multiple molecular species, each species being replicated in a
211 template-based manner while helping the replication of other members of the network. The resulting
212 cooperative dynamics can raise the error threshold, thereby increasing the replicase regime zone
213 (Takeuchi, Hogeweg and Kaneko, 2017). Other scenarios introduce compartments and more generally
214 spatial structure. The Stochastic Corrector Model (SCM) considers lineages of compartments which
215 grow, are selected, and divide (Szathmary and Demeter, 1987; Grey, Hutson and Szathmary, 1995).
216 Transient Compartmentalization (TC) assumes simpler cycles consisting of compartmentalization,
217 selection, and pooling (Matsumura *et al.*, 2016; Blokhuis *et al.*, 2020). Unlike the original model and
218 its equation (1), SCM and TC authorize the presence of parasite sequences that replicate faster than
219 the reference sequence. This was experimentally demonstrated for TC with replicated RNA
220 (Matsumura *et al.*, 2016). Indeed, in both cases, erroneous copies only locally invade compartments
221 and are removed from the population by compartment-level selection. Surface clusters are an even
222 less constrained setting that allows the maintenance of replication, although less efficiently than non-
223 permeable compartments (Szabo *et al.*, 2002; Shah *et al.*, 2019). These mechanisms increase e_{max} ,
224 thus also increase the plausibility of the replicase scenario. However, this comes at the cost of
225 assuming the existence of spatial structures and introducing additional parameters (number of
226 molecules per compartment, compartment lifetime, selection process, etc.).

227 Once the error threshold is determined, the next question is to estimate the fraction of viable
228 replicases in the sequence space. This corresponds to determining the distribution f in equation (2),
229 which depends on the relationship between sequence and catalytic function, including the minimum
230 possible error rate e_{min} given a certain replicase length. This problem cannot be solved
231 computationally yet, and heavily relies on experimental data. Experiments on synthetic replicases
232 show that processivity — the ability to copy long templates — is a limiting factor even before
233 considering fidelity. Processivity is notably hampered when copying folded RNAs, which is the case
234 for replicase templates. Consistently, replicases synthesized in the laboratory can copy other RNAs as
235 long as themselves but cannot copy themselves (Horning and Joyce, 2016; Attwater *et al.*, 2018).

236 Another issue is that the sequence space cannot be covered experimentally due to its astronomical size
237 ($\sim 10^{14}$ for a typical 190 nucleotides long replicase (Johnston *et al.*, 2001)). Consequently,
238 experimental data need to be combined with theory and computation in order to estimate f . For
239 instance, the diversity of RNA secondary structures is predicted to increase as $1.4848 \times$
240 $n^{-\frac{3}{2}}(1.8488)^n$ where n is the sequence length (Schuster *et al.*, 1994). This is consistently smaller
241 than the 4^n possible sequences. Taking structure similarity as a proxy for function indicates an
242 average redundancy in sequences with similar catalytic properties, potentially reducing the size of the
243 space to characterize. A complementary approach is to estimate the tail of distribution f between e_{min}
244 and e_{max} (figure 2.d) using laws of extreme statistics (Gumbel, 1958). Indeed, replicases are rare
245 sequences for which statistics are expected to follow extreme value theory. The latter restricts
246 distributions of rare properties to functional forms (among the Weibull, Gumbel and Fréchet laws)
247 with few parameters. Such approach has been tested experimentally for proteins (Boyer *et al.*, 2016)
248 and ribozymes (Pressman *et al.*, 2017). Despite the complexity of the genotype-to-phenotype
249 relationship, the limited number of parameters involved in these laws may allow estimates of f from a
250 restricted sample of replicases.

251 Finally, the transition scenario toward existence of a sustainable replicase may be revised by
252 considering different polymer generation processes anterior to the replicase regime. Polymer
253 generation could have been enhanced by catalysis of polymerization (Hazen and Sverjensky, 2010),
254 ligation (Mutschler *et al.*, 2018), or recombination (Blokhuys and Lacoste, 2017), as well as by size
255 selection (Mizuuchi *et al.*, 2019). An alternative is that autocatalytic sets could have preceded
256 template-based replication and biased polymer populations toward longer and more functional
257 sequences (Vasas *et al.*, 2012). All these processes can add weight to the distribution g in equation (2)
258 in the length categories corresponding to replicases and contribute to the plausibility of their
259 emergence.

260 4. Generalizing the threshold approach

261 We have seen that the error threshold sets a number of requirements on polymerases for them to
262 sustain replication. We now generalize the threshold approach to other properties of prebiotic systems.
263 In figure 3, the axes correspond to relevant parameters of the system and its environment, and regions
264 α and β respectively correspond to systems without and with a property of interest (regions separated
265 by a threshold line). We call this representation a phase diagram, by analogy with equilibrium
266 thermodynamics, extending its use to non-equilibrium regimes as well. In the replicase scenario,
267 region α corresponds to a regime of randomly produced RNAs and region β to sustainable template-
268 based RNA replication, the boundary between the two being the error threshold. In contrast with
269 figure 2 where the axes stand for system parameters only, the x-axis in figure 3 captures system
270 parameters (e.g. replicase error rate) and the y-axis environment variables (e.g. temperature). Note
271 that it is not always obvious to distinguish prebiotic systems from their environment, and choosing a
272 variable as being either part of the system or of the environment may be a matter of choice. Note also
273 that the x-axis represents chosen control parameters of the system; other parameters of the system
274 may lie in other dimensions, in particular as encoded by the green shading of β in figure 3, which
275 indicates the presence of a specific property of the system. A point in the diagram then represents a
276 system with certain fixed properties in a given environment. Such phase diagrams allow us to classify
277 modes by which a system overcomes a threshold and acquires a novel property, i.e. moves from
278 region α to region β . We classify transitions into four modes:

279 1. *Extrinsic transition*: the acquisition of a new property is here solely driven by the environment. In
280 figure 3a, the system is initially located at point A in region α and environment E_1 ; a change from E_1
281 to E_2 brings the system to B in region β . Since this transition is not caused by any change in the
282 system control parameters, there is no variation along the x-axis. Transitions in prebiotic chemistry
283 are typically framed in the context of extrinsic transitions (Kawamura and Maurel, 2017; Kitadai and
284 Maruyama, 2018; Benner *et al.*, 2019), where concentration thresholds are overcome during wet-dry
285 cycles in ponds (Campbell *et al.*, 2019), where steps of nucleobase synthesis occur at the junction of
286 interconnecting streams (Patel *et al.*, 2015), or where hydrogen cyanide is synthesized upon meteorite
287 impacts (Parkos *et al.*, 2018). This mode can also be applied to the appearance of vesicles triggered
288 by CO_2 (Bachmann, Luigi and Lang, 1992).

289 2. *Intrinsic transition*: the novel property here results from changes in parameters of the system while
290 the environment remains unchanged. In figure 3.b, the system is initially located at point A in α with
291 environment E_1 , and moves to B in β without any environmental change, simply moving along the x-
292 axis. This is the case when a replicase appears from random polymerization as described in section 3
293 (Mathis, Bhattacharya and Walker, 2017). Another example is the appearance of autocatalytic sets as
294 modelled by Jain and Krishna (1998). This model assumes that catalytic species only are limiting and
295 follow a dynamic where the least fit species tend to disappear and be randomly replaced by novel
296 catalytic species. Under these assumptions, an autocatalytic set inevitably emerges and fixes. Note
297 that in the examples cited above, extrinsic transitions are deterministic while intrinsic transitions are
298 stochastic, but this need not always be the case. For a discussion on contingency versus determinism
299 in the origin of life see Luisi (2003).

300 3. *Scaffolding transition*: the environment changes only transiently, and fixing a novel property
301 requires to combine the environmental change with a system-driven change. Here, the environment
302 plays the role of a scaffold in the sense that it transiently supports the emergence of a property which
303 is then internalized, i.e. becomes an intrinsic property of the system (Caporael, Griesemer and
304 Wimsatt, 2014). In figure 3c, the system starts at point A in region α in environment E_1 , then moves to
305 point B in region β via an extrinsic transition triggered by an environmental change to E_2 . At this
306 stage, returning to E_1 would bring the system back into α . However, if the property acquired in β
307 allows exploration of neighboring areas along the x-axis, the system may reach B' in β while in
308 environment E_2 . Then, an environmental change from E_2 back to E_1 would bring the system from B'
309 to B'', yet still within β . Such scaffolding transition could be observed when a dilute solution of
310 polymers in a pond (system in A) is submitted to partial evaporation (from E_1 to E_2), thereby reaching
311 a concentration threshold above which autocatalysis becomes possible (system in B), leading it to
312 accumulate enough catalysts (from B to B') so that once back to wet conditions, autocatalysis is
313 maintained (from B' to B'').

314 4. *Symbiotic transition*: two distinct systems aggregate into a new system thereby acquiring a novel
315 property. In figure 3.d, systems A and B both in α merge into a new system C located in β in a
316 constant environment. Such transition is hypothesized when compartments meet autocatalytic
317 chemistries (Hordijk *et al.*, 2018; Joyce and Szostak, 2018). Both may pre-exist separately, but
318 evolution by natural selection requires autocatalytic chemistries to be compartmentalized in order to
319 provide a collective level of selection (Vasas *et al.*, 2012).

320

321 5. Articulating series of thresholds

322 In previous sections, we analyzed single threshold transitions. However, origin of life scenarios
323 combine multiple transitions (Szathmáry, 2015; Solé, 2016). There are to date only a few attempts to
324 assemble complete detailed scenarios (Martin *et al.*, 2003; Damer and Deamer, 2020). Research
325 efforts have focused on combining transitions for specific stages, such as the synthesis of building
326 blocks (Patel *et al.*, 2015; Kitadai and Maruyama, 2018; Becker *et al.*, 2019), the emergence of
327 functional RNAs from random ones (Briones, Stich and Manrubia, 2009; Higgs and Lehman, 2015) or
328 the emergence of evolution from catalytic micelles (Lancet, Zidovetzki and Markovitch, 2018), to cite
329 a few. Below, we apply the phase diagram representation to multiple thresholds. This analysis reveals
330 different types of articulations between threshold transitions: *accumulation*, *entrenchment*,
331 *contingency*, *transience*, *facilitation*. These concepts are borrowed from evolutionary biology but are
332 used here to analyze systems that do not necessarily evolve in a Darwinian manner. We indeed
333 consider these concepts to be generally applicable to successions of threshold transitions, heritable
334 transitions through Darwinian evolution only being a particular case.

335 We first consider the crossing of two successive thresholds. In figures 4.a-c, the green and blue
336 regions β and γ indicate systems which possess properties p_β and p_γ , respectively; in region α , the
337 system does not possess any of them. Here, the x- and y-axes depict relevant variables that can be
338 environmental, systemic or both. For *accumulation* of properties p_β and p_γ to be possible, regions β
339 and γ must intersect. Figures 4a-c depict systems that start from region α , then cross the threshold
340 leading to β , followed by a second threshold-crossing to region γ . A notion stronger than
341 accumulation is *entrenchment*, where any property p_γ posterior to p_β requires it and fixes it
342 irreversibly. This is illustrated in figure 4a, where region γ is entirely included in region β . For
343 example, p_β could stand for the existence of catalytic RNAs and p_γ of autocatalytic RNAs. Another
344 threshold articulation is when β and γ intersect without inclusion. Such a situation is characterized by
345 *contingency* in the sense that p_γ may exist independently of p_β (and vice-versa) so that any of the two
346 properties may appear first (figure 4.b, from points A to B or points A to b). This would be the case
347 with the appearance of RNAs (p_γ) together with other genetic polymers (p_β) (Cleaves *et al.*, 2019).
348 Alternative polymers further illustrate *transience*, where a property is acquired, and then lost (figure
349 4.b, any path from point A to point D). For instance, TNA may have appeared, coexisted with RNA,
350 then disappeared (Yu, Zhang and Chaput, 2012). Finally, a threshold transition can make a subsequent
351 transition more plausible when acquiring p_β lowers the threshold to acquire p_γ (figure 4.c); this is
352 referred to as *facilitation*. For example, compartmentalization (p_β) lowers the error threshold that
353 delineates sustainable replication (p_γ) (Matsumura *et al.*, 2016).

354 We now consider the articulation between more than two thresholds as depicted in figure 4.d as a
355 Venn diagram, where thresholds delineate regions corresponding to different properties. For example,
356 a chemical system may start in region α where it has the ability to synthesize random RNAs. By
357 reaching β , it gains the ability to synthesize random peptides as well. Next, reaching γ allows
358 autocatalysis among sets of peptides. Furthermore, in these examples, the system is allowed to
359 *accumulate* the properties that define α , β and γ because they all intersect. An example of
360 *entrenchment* here is RNA oligomer synthesis (α) that is a necessary condition for the existence of
361 autocatalysis in RNA sets (δ is fully included in α). *Transience* happens if the system loses its ability
362 to synthesize random RNAs (α) but acquires protein RNA-replicases (ϕ), as it allows replication of
363 long RNAs from single nucleotides.

364 The notion of *entrenchment* can be further refined. As we have seen, it occurs when a system cannot
365 get rid of a feature because too many features have evolved on that basis. As a result, the entrenched
366 feature can narrow down the access to other properties as well as open other possibilities. The former
367 is known as “contingent irreversibility” (Smith and Szathmáry, 1995) and the latter as “generative
368 entrenchment” (Schank and Wimsatt, 1986) or “enabling constraint” (Kauffman, 2014). In figure 4.d,
369 reaching region δ allows transition to region ϵ but not ϕ . The advent of homochirality illustrates these
370 notions. Indeed, a racemic mixture of oligonucleotides (region β in figure 4.d) could break its
371 symmetry because of a triggered small enantiomeric excess amplified by an autocatalytic reaction
372 leading either to L-ribose RNA only (region γ) either to D-ribose RNA only (region δ) (Hawbaker and
373 Blackmond, 2019). Entrenchment would follow with peptide synthesis: L-ribose RNA systems could
374 imply D-amino acids peptides only (region ϕ) whereas D-ribose RNA systems could imply L-amino
375 acids peptides only (region ϵ) (Illangasekare *et al.*, 2010).

376 Finally, we relate the diagram representations to the concept of *lifeness* (also referred as *aliveness* or
377 *life index*) proposed by several authors (Bruylants, Bartik and Reisse, 2010; Sutherland, 2017;
378 Malaterre and Chartier, 2019). Lifeness stands for a scale where so-called “infrabiological systems”
379 (Szathmáry, 2005) are positioned between a non-living state and a living state. It remains unclear
380 which quantities or measures best account for lifeness. For instance, Bedau (2012) proposes a discrete
381 scale from 0 to 9 depending on the number of interactions between three subsystems: container,
382 metabolism and program, while Malaterre and Chartier (2019) propose a multidimensional gradual
383 scale that integrates system and environment-related functions. In any case, projecting the paths of
384 figure 4d on any such measure would make threshold transitions appear as jumps, the directionality of
385 paths towards a living state corresponding to increasing lifeness (figure 4.e). In this view, we propose
386 that lifeness corresponds, at first order, to the number of thresholds crossed relative to the total
387 number of thresholds in a given scenario. This suggests a way toward formalizing the notion of
388 chemical evolution: early prebiotic systems may not yet evolve in a canonically Darwinian manner,
389 but in the sense of acquiring and sustaining qualitatively novel properties by crossing thresholds,
390 thereby increasing their lifeness before getting a chance to increasing their fitness.

391

392 6. Discussion

393

394 Thresholds define conditions of existence for particular states along the path from inanimate matter to
395 life. Although not all prebiotic transitions are threshold transitions, thresholds pose well-defined
396 problems that can structure interdisciplinary efforts to understand the origin of life (Fig. 5).
397 Thresholds may initially be deduced from apparent paradoxes, so-called “catch-22” or “chicken-and-
398 egg” situations stated as: “without X, no Y, and without Y, no X” (Benner, 2018). For instance, from
399 a bird’s-eye view of life, metabolism, genetics and compartments appear so intertwined that there is
400 no obvious scenario for their gradual emergence. As we have seen, thresholds are also detected when
401 taking a closer look at molecular processes, such as template-based replication, or from computer
402 simulations and experiments. Their signatures are discontinuities, hysteresis and waiting time
403 distributions, as observed with first order phase transitions in physics.

404

405 Quantitatively characterizing a threshold requires back-and-forth adjustments between theory and
406 experiment. Interestingly, thresholds pose conditions of existence of a given state without referring to
407 an anterior nor a posterior state. Thus, their study is independent of a particular transition or scenario

408 in the first place. The starting point is typically a simplified model establishing relationships between
409 parameters. Such a “toy-model” has been highly productive in the case of the error threshold, notably
410 pointing to the disciplinary diversity of its parameters. From this point, thorough theoretical
411 investigations of the parameter space and regimes help elaborating hypotheses testable with synthetic
412 experiments in chemistry, systems chemistry, physical-chemistry, soft matter physics, etc. (Solé,
413 2016; Preiner *et al.*, 2019). In turn, models may be refined until convergence. A possible outcome is
414 that the proposed regime is impossible due to multiple incompatible thresholds, resulting in a true
415 paradox and the revision of the scenario with alternative regimes. Otherwise, the regime is possible
416 and then comes the question of its plausibility.

417
418 To assess plausibility, transition from an anterior state must be accounted for (Orgel, 2008; Schwartz,
419 2013). Theory, possibly again with back-and-forth adjustment with experiments, estimates the
420 probability of crossing the threshold given the anterior state and environmental conditions as
421 determined by geology, geochemistry, or planetary dynamics (Stüeken *et al.*, 2013; Sasselov,
422 Grotzinger and Sutherland, 2020). Comparing the crossing probability from different anterior states
423 and environments selects between transitions (e.g. random polymerization or autocatalytic sets before
424 to template-based replication). The plausibility of scenarios finally results from the probability of
425 successions of such transitions. If this total probability is deemed too low, alternative scenarios may
426 lead to consider novel thresholds (e.g. error thresholds with compartment instead of without).

427
428 So far, no one agrees on whether any scenario is devoid of true paradoxes (impossibilities). However,
429 the threshold approach outlined above can establish firm building blocks on the way to constructing
430 scenarios. For this to be effective, studies on the origin of life ought to be explicit with the thresholds
431 they address, the parameters involved, and the relationships between these parameters, following the
432 example of the error threshold.

433

434 Resource availability

435 **Lead Contact**

436

437 Further information and requests for resources should be directed to and will be fulfilled by the Lead
438 Contact Philippe Nghe (philippe.nghe@espci.psl.eu)

439

440 **Materials Availability**

441

442 This study did not use or generate any reagents

443

444 **Data and Code Availability**

445

446 This study did not use any dataset or code

447

448 Acknowledgments

449 The authors thank the Origines et Conditions d'Apparition de la Vie (OCAV) IRIS initiative at PSL
450 Research University for stimulating discussions. The manuscript also benefited from the comments of
451 two anonymous reviewers for *iScience*. CJ acknowledges financial support by Université de Paris and
452 the École Doctorale FIRE - Programme Bettencourt. This work has received the support of "Institut
453 Pierre-Gilles de Gennes" (laboratoire d'excellence, "Investissements d'avenir" program ANR-10-
454 IDEX-0001-02 PSL and ANR-10-LABX-31). PN acknowledges funding from the Human Frontier
455 Science Program (Grant RGY0077/2019). CM acknowledges funding from an ESPCI Joliot Chair,
456 Canada Social Sciences and Humanities Research Council [Grant 430-2018-00899] and Canada
457 Research Chairs [CRC-950-230795].

458 Author Contributions

459 All authors contributed equally to this study.

460 Declaration of Interest

461 The authors declare no competing interests.

462 References

- 463
464 Arnoldt, H., Strogoz, S. H. and Timme, M. (2015) 'Toward the Darwinian transition: Switching between distributed and
465 speciated states in a simple model of early life', *Physical Review E*, 92(5), pp. 1–9. doi: 10.1103/PhysRevE.92.052909.
466 Attwater, J. *et al.* (2018) 'Ribozyme-catalysed RNA synthesis using triplet building blocks', *eLife*, 7, pp. 1–25. doi:
467 10.7554/eLife.35255.
468 Attwater, J. and Holliger, P. (2014) 'A synthetic approach to abiogenesis', *Nature Methods*. Nature Publishing Group, 11(5),
469 pp. 495–498. doi: 10.1038/nmeth.2893.
470 Baaske, P. *et al.* (2007) 'Extreme accumulation of nucleotides in simulated hydrothermal pore systems', *Proceedings of the*
471 *National Academy of Sciences of the United States of America*, 104(22), pp. 9346–9351. doi: 10.1073/pnas.0609592104.
472 Bachmann, P. A., Luigi, P. and Lang, J. (1992) 'Micelles As Models for Prebiotic Structures', *Nature*, 357(May), pp. 1013–
473 1015.
474 Becker, S. *et al.* (2019) 'Unified prebiotically plausible synthesis of pyrimidine and purine RNA ribonucleotides', *Science*,
475 366(6461), pp. 76–82. doi: 10.1126/science.aax2747.
476 Bedau, M. A. (2012) 'A functional account of degrees of minimal chemical life', *Synthese*, 185(1), pp. 73–88. doi:
477 10.1007/s11229-011-9876-x.
478 Benner, S. A. (2018) 'Prebiotic plausibility and networks of paradox-resolving independent models', *Nature*
479 *Communications*. Springer US, 9(1), pp. 9–11. doi: 10.1038/s41467-018-07274-y.
480 Benner, S. A. *et al.* (2019) 'When Did Life Likely Emerge on Earth in an RNA-First Process?', *ChemSystemsChem*,
481 1900035. doi: 10.1002/syst.201900035.
482 Blokhuis, A. *et al.* (2020) 'The generality of transient compartmentalization and its associated error thresholds', *Journal of*
483 *Theoretical Biology*. Elsevier Ltd, 487, p. 110110. doi: 10.1016/j.jtbi.2019.110110.
484 Blokhuis, A. and Lacoste, D. (2017) 'Length and sequence relaxation of copolymers under recombination reactions', *The*
485 *Journal of Chemical Physics*. AIP Publishing LLC, 147(9), p. 094905. doi: 10.1063/1.5001021.
486 Blokhuis, A., Lacoste, D. and Nghe, P. (2020) 'Universal motifs and the diversity of autocatalytic systems', *Proceedings of*
487 *the National Academy of Sciences*. doi: 10.1073/pnas.2013527117.
488 Boulanger, E. *et al.* (2013) 'Photochemical Steps in the Prebiotic Synthesis of Purine Precursors from HCN', *Angewandte*
489 *Chemie*, 125(31), pp. 8158–8161. doi: 10.1002/ange.201303246.
490 Boyer, S. *et al.* (2016) 'Hierarchy and extremes in selections from pools of randomized proteins', *Proceedings of the*
491 *National Academy of Sciences of the United States of America*, 113(13), pp. 3482–3487. doi: 10.1073/pnas.1517813113.
492 Briones, C., Stich, M. and Manrubia, S. C. (2009) 'The dawn of the RNA World: Toward functional complexity through
493 ligation of random RNA oligomers', *RNA*, 15, pp. 743–749. doi: 10.1261/rna.1488609.Orgel.
494 Bruylants, G., Bartik, K. and Reisse, J. (2010) 'Prebiotic chemistry: A fuzzy field', *Comptes Rendus Chimie*. Academie des

495 sciences, 14(4), pp. 388–391. doi: 10.1016/j.crci.2010.04.002.

496 Budin, I. and Szostak, J. W. (2010) ‘Expanding Roles for Diverse Physical Phenomena During the Origin of Life’, *Annual*

497 *Review of Biophysics*, 39(1), pp. 245–263. doi: 10.1146/annurev.biophys.050708.133753.

498 Campbell, T. D. *et al.* (2019) ‘Prebiotic condensation through wet–dry cycling regulated by deliquescence’, *Nature*

499 *Communications*. Springer US, 10, p. 4508. doi: 10.1038/s41467-019-11834-1.

500 Caporael, L. R., Griesemer, J. R. and Wimsatt, W. C. (2014) ‘Developing scaffolds: An introduction’, in *Developing*

501 *scaffolds in evolution, culture, and cognition*, pp. 1–20.

502 Carny, O. and Gazit, E. (2005) ‘A model for the role of short self-assembled peptides in the very early stages of the origin of

503 life’, *The FASEB Journal*, 19(9), pp. 1051–1055. doi: 10.1096/fj.04-3256hyp.

504 Chen, I. A. and Nowak, M. A. (2012) ‘From Pre-life to Life: How Chemical Kinetics Become Evolutionary Dynamics’,

505 *Accounts of Chemical Research*, 45(12). doi: 10.1021/ar2002683.

506 Cheng, L. K. L. and Unrau, P. J. (2010) ‘Closing the circle: replicating RNA with RNA.’, *Cold Spring Harbor perspectives*

507 *in biology*. Cold Spring Harbor Laboratory Press, 2(10), p. a002204. doi: 10.1101/cshperspect.a002204.

508 Claverys, J.-P., Prudhomme, M. and Martin, B. (2006) ‘Induction of Competence Regulons as a General Response to Stress

509 in Gram-Positive Bacteria’, *Annual Review of Microbiology*, 60(1), pp. 451–475. doi:

510 10.1146/annurev.micro.60.080805.142139.

511 Cleaves, H. J. *et al.* (2019) ‘One among Millions: The Chemical Space of Nucleic Acid-Like Molecules’, *Journal of*

512 *Chemical Information and Modeling*. doi: 10.1021/acs.jcim.9b00632.

513 Cohen, J. E. (1988) ‘Threshold phenomena in random structures’, *Discrete Applied Mathematics*, 19(1–3), pp. 113–128. doi:

514 10.1016/0166-218X(88)90008-X.

515 Damer, B. and Deamer, D. (2020) ‘The hot spring hypothesis for an origin of life’, *Astrobiology*, 20(4), pp. 429–452. doi:

516 10.1089/ast.2019.2045.

517 Dickson, K. S., Burns, C. M. and Richardson, J. P. (2000) ‘Determination of the free-energy change for repair of a DNA

518 phosphodiester bond’, *Journal of Biological Chemistry*, 275(21), pp. 15828–15831. doi: 10.1074/jbc.M910044199.

519 de Duve, C. (1991) *Blueprint for a cell: The nature and origin of life*. Burlington: Patterson.

520 Eigen, M. (1971) ‘Selforganization of matter and the evolution of biological macromolecules’, *Die Naturwissenschaften*,

521 58(10), pp. 465–523. doi: 10.1007/BF00623322.

522 Eigen, M., McCaskill, J. and Schuster, P. (1988) ‘Molecular quasi-species’, *Journal of Physical Chemistry*, 92(24), pp.

523 6881–6891. doi: 10.1021/j100335a010.

524 Eigen, M. and Schuster, P. (1977) ‘The Hypercycle A Principle of Natural Self-Organization’, *Die Naturwissenschaften*, 64,

525 pp. 541–565. doi: 10.1007/978-3-642-67247-7_1.

526 Eschenmoser, A. and Loewenthal, E. (1991) ‘Chemistry of Potentially Prebiological Natural Products’, *Chemical Society*

527 *Reviews*, 67(281), pp. 1–16.

528 Farmer, J. D., Kauffman, S. A. and Packard, N. H. (1986) ‘Autocatalytic replication of polymers’, *Physica*, 220, pp. 50–67.

529 Gartner, F. M. *et al.* (2020) ‘Stochastic yield catastrophes and robustness in self-assembly’, *eLife*, 9. doi:

530 10.7554/elife.51020.

531 Goldenfeld, N., Biancalani, T. and Jafarpour, F. (2017) ‘Universal biology and the statistical mechanics of early life’,

532 *Philosophical Transactions of the Royal Society A*, 375(2109). doi: 10.1098/rsta.2016.0341.

533 Grey, D., Hutson, V. and Szathmari, E. (1995) ‘A re-examination of the stochastic corrector model’, *Proceedings of the*

534 *Royal Society B: Biological Sciences*, 262(1363), pp. 29–35. doi: 10.1098/rspb.1995.0172.

535 Gumbel, E. J. (1958) *Statistics of Extremes*. New-York: Columbia University Press.

536 Hargreaves, W. R., Mulvihill, S. J. and Deamer, D. W. (1977) ‘Synthesis of phospholipids and membranes in prebiotic

537 conditions’, *Nature*, 266(5597), pp. 78–80. doi: 10.1038/266078a0.

538 Hawbaker, N. A. and Blackmond, D. G. (2019) ‘Energy threshold for chiral symmetry breaking in molecular self-

539 replication’, *Nature Chemistry*. Springer US, 11(10), pp. 957–962. doi: 10.1038/s41557-019-0321-y.

540 Hazen, R. M. and Sverjensky, D. A. (2010) ‘Mineral Surfaces, Geochemical Complexities, and the Origins of Life’, *Cold*

541 *Spring Harbor Perspectives in Biology*, 2, p. a002162. doi: 10.1016/0169-5347(88)90031-6.

542 Higgs, P. G. and Lehman, N. (2015) ‘The RNA World: Molecular cooperation at the origins of life’, *Nature Reviews*

543 *Genetics*. Nature Publishing Group, 16(1), pp. 7–17. doi: 10.1038/nrg3841.

544 Hordijk, W. *et al.* (2018) ‘Population Dynamics of Autocatalytic Sets in a Compartmentalized Spatial World’, *Life*, 8(3), p.

545 33. doi: 10.3390/life8030033.

546 Horning, D. P. and Joyce, G. F. (2016) ‘Amplification of RNA by an RNA polymerase ribozyme’, *Proceedings of the*

547 *National Academy of Sciences*, 113(35), pp. 9786–9791. doi: 10.1073/pnas.1610103113.

548 Ichihashi, N. and Yomo, T. (2016) ‘Constructive approaches for understanding the origin of self-replication and evolution’,

549 *Life*, 6(3), pp. 1–12. doi: 10.3390/life6030026.

550 Illangasekare, M. *et al.* (2010) ‘Chiral histidine selection by D-ribose RNA’, *Rna*, 16(12), pp. 2370–2383. doi:

551 10.1261/rna.2385310.

552 Jain, S. and Krishna, S. (1998) ‘Autocatalytic sets and the growth of complexity in an evolutionary model’, *Physical Review*

553 *Letters*, 81(25), pp. 5684–5687. doi: 10.1103/PhysRevLett.81.5684.

554 Jiang, H. *et al.* (2015) ‘Phase Transition of Spindle-Associated Protein Regulate Spindle Apparatus Assembly’, *Cell*.

555 Elsevier Inc., 163(1), pp. 108–122. doi: 10.1016/j.cell.2015.08.010.

556 Johnston, W. K. *et al.* (2001) ‘RNA-catalyzed RNA polymerization: Accurate and general RNA-templated primer

557 extension’, *Science*, 292(5520), pp. 1319–1325. doi: 10.1126/science.1060786.

558 Joyce, G. F. and Szostak, J. W. (2018) ‘Protocells and RNA Self-Replication’, *Cold Spring Harbor Perspectives in Biology*.

559 Cold Spring Harbor Laboratory Press, 10(9), p. a034801. doi: 10.1101/CSHPERSPECT.A034801.

560 Kauffman, S. A. (1986) ‘Autocatalytic sets of proteins’, *Journal of Theoretical Biology*, 119(1), pp. 1–24. doi:

561 10.1016/S0022-5193(86)80047-9.

562 Kauffman, S. A. (1993) *The Origins of Order: Self-Organization and Selection in Evolution*. Oxford University Press.

563 Kauffman, S. A. (2014) 'Prolegomenon to patterns in evolution', *BioSystems*. Elsevier Ireland Ltd, 123, pp. 3–8. doi:

564 10.1016/j.biosystems.2014.03.004.

565 Kawamura, K. and Maurel, M. C. (2017) 'Walking over 4 Gya: Chemical Evolution from Photochemistry to Mineral and

566 Organic Chemistries Leading to an RNA World', *Origins of Life and Evolution of Biospheres*. Origins of Life and Evolution

567 of Biospheres, 47(3), pp. 281–296. doi: 10.1007/s11084-017-9537-2.

568 King, G. A. M. (1977) 'Symbiosis and the origin of life', *Origins of Life*, 8, pp. 39–53. doi: 10.1201/9780203009918.

569 Kitadai, N. and Maruyama, S. (2018) 'Origins of building blocks of life: A review', *Geoscience Frontiers*. Elsevier, 9(4), pp.

570 1117–1153. doi: 10.1016/j.gsf.2017.07.007.

571 Kovács, Á. T. *et al.* (2009) 'Ubiquitous late competence genes in *Bacillus* species indicate the presence of functional DNA

572 uptake machineries: Minireview', *Environmental Microbiology*, 11(8), pp. 1911–1922. doi: 10.1111/j.1462-

573 2920.2009.01937.x.

574 Kun, Á. *et al.* (2015) 'The dynamics of the RNA world: Insights and challenges', *Annals of the New York Academy of*

575 *Sciences*, 1341(1), pp. 75–95. doi: 10.1111/nyas.12700.

576 Kun, Á., Santos, M. and Szathmáry, E. (2005) 'Real ribozymes suggest a relaxed error threshold', *Nature Genetics*, 37(9),

577 pp. 1008–1011. doi: 10.1038/ng1621.

578 Lambert, J. F. (2008) 'Adsorption and polymerization of amino acids on mineral surfaces: A review', *Origins of Life and*

579 *Evolution of Biospheres*, 38(3), pp. 211–242. doi: 10.1007/s11084-008-9128-3.

580 Lancet, D., Zidovetzki, R. and Markovitch, O. (2018) 'Systems protobiology: Origin of life in lipid catalytic networks',

581 *Journal of the Royal Society Interface*, 15(144). doi: 10.1098/rsif.2018.0159.

582 Luisi, P. L. (2003) 'Contingency and determinism', *Philosophical Transactions of the Royal Society A: Mathematical,*

583 *Physical and Engineering Sciences*, 361(1807), pp. 1141–1147. doi: 10.1098/rsta.2003.1189.

584 Luisi, P. L., Stano, P. and de Souza, T. (2014) 'Spontaneous Overcrowding in Liposomes as Possible Origin of Metabolism',

585 *Origins of Life and Evolution of Biospheres*, 44(4), pp. 313–317. doi: 10.1007/s11084-014-9387-0.

586 Malaterre, C. and Chartier, J.-F. (2019) 'Beyond categorical definitions of life: a data-driven approach to assessing lifeness',

587 *Synthese*. Springer Netherlands. doi: 10.1007/s11229-019-02356-w.

588 Martin, W. *et al.* (2003) 'On the origins of cells: A hypothesis for the evolutionary transitions from abiotic geochemistry to

589 chemoautotrophic prokaryotes, and from prokaryotes to nucleated cells', *Philosophical Transactions of the Royal Society B:*

590 *Biological Sciences*, 358(1429), pp. 59–85. doi: 10.1098/rstb.2002.1183.

591 Mathis, C., Bhattacharya, T. and Walker, S. I. (2017) 'The Emergence of Life as a First-Order Phase Transition',

592 *Astrobiology*, 17(3), pp. 266–276. doi: 10.1089/ast.2016.1481.

593 Matsumura, S. *et al.* (2016) 'Transient compartmentalization of RNA replicators prevents extinction due to parasites',

594 *Science*, 354(6317), pp. 1293–1296.

595 Miller, S. L. (1953) 'A production of amino acids under possible primitive earth conditions', *Science*, 117(3046), pp. 528–

596 529. doi: 10.1126/science.117.3046.528.

597 Miyakawa, S., Cleaves, H. J. and Miller, S. L. (2002) 'the Cold Origin of Life : Hydrogen Cyanide and Formamide', *Origins*

598 *of Life and Evolution of the Biosphere*, 32(1986), pp. 195–208.

599 Mizuuchi, R. *et al.* (2019) 'Mineral surfaces select for longer RNA molecules', *Chemical Communications*. Royal Society of

600 Chemistry, 55(14), pp. 2090–2093. doi: 10.1039/c8cc10319d.

601 Monnard, P. A., Kanavarioti, A. and Deamer, D. W. (2003) 'Eutectic Phase Polymerization of Activated Ribonucleotide

602 Mixtures Yields Quasi-Equimolar Incorporation of Purine and Pyrimidine Nucleobases', *Journal of the American Chemical*

603 *Society*, 125(45), pp. 13734–13740. doi: 10.1021/ja036465h.

604 Mutschler, H. *et al.* (2018) 'Random-sequence genetic oligomer pools display an innate potential for ligation and

605 recombination', *eLife*, 7, pp. 1–26. doi: 10.7554/eLife.43022.

606 Nelson, K. E. *et al.* (2001) 'Concentration by Evaporation and the prebiotic Synthesis of Cytosine', *Origins of Life and*

607 *Evolution of the Biosphere*, 31(3), pp. 221–229. doi: 10.1023/A:1016582308525.

608 Obermayer, B. and Frey, E. (2009) 'Escalation of error catastrophe for enzymatic self-replicators', *Europhysics Letters*,

609 88(4). doi: 10.1209/0295-5075/88/48006.

610 Oparin, A. I. (1938) *The Origin of Life*. New-York: Macmillan Publishers Limited.

611 Orgel, L. E. (2008) 'The implausibility of metabolic cycles on the prebiotic earth', *PLoS Biology*, 6(1), pp. 0005–0013. doi:

612 10.1371/journal.pbio.0060018.

613 Parkos, D. *et al.* (2018) 'HCN Production via Impact Ejecta Reentry During the Late Heavy Bombardment', *Journal of*

614 *Geophysical Research: Planets*, 123(4), pp. 892–909. doi: 10.1002/2017JE005393.

615 Pascal, R. (2012) 'Suitable energetic conditions for dynamic chemical complexity and the living state', *Journal of Systems*

616 *Chemistry*, 3(1), pp. 1–5. doi: 10.1186/1759-2208-3-3.

617 Patel, B. H. *et al.* (2015) 'Common origins of RNA, protein and lipid precursors in a cyanosulfidic protometabolism', *Nature*

618 *Chemistry*. Nature Publishing Group, 7(4), pp. 301–307. doi: 10.1038/nchem.2202.

619 Poole, A. M. (2009) 'Horizontal gene transfer and the earliest stages of the evolution of life', *Research in Microbiology*.

620 Elsevier Masson SAS, 160(7), pp. 473–480. doi: 10.1016/j.resmic.2009.07.009.

621 Preiner, M. *et al.* (2019) 'The future of origin of life research: bridging decades-old divisions', *Life*, (January), p. under

622 review. doi: 10.3390/life10030020.

623 Pressman, A. *et al.* (2017) 'Analysis of in vitro evolution reveals the underlying distribution of catalytic activity among

624 random sequences', *Nucleic Acids Research*, 45(14), pp. 8167–8179. doi: 10.1093/nar/gkx540.

625 Rimmer, P. B. *et al.* (2018) 'The origin of RNA precursors on exoplanets', *Science Advances*, 4(8), pp. 1–12. doi:

626 10.1126/sciadv.aar3302.

627 Sasselov, D. D., Grotzinger, J. P. and Sutherland, J. D. (2020) 'The origin of life as a planetary phenomenon', *Science*

628 *Advances*, 6(6), pp. 1–10. doi: 10.1126/sciadv.aax3419.

629 Schank, J. C. and Wimsatt, W. C. (1986) 'Generative Entrenchment and Evolution', *Proceedings of the Biennial Meeting of*
630 *the Philosophy of Science Association*, 2, pp. 33–60.

631 Schuster, P. *et al.* (1994) 'From sequences to shapes and back: A case study in RNA secondary structures', *Proceedings of*
632 *the Royal Society B: Biological Sciences*, 255(1344), pp. 279–284. doi: 10.1098/rspb.1994.0040.

633 Schwartz, A. W. (2013) 'Evaluating the plausibility of prebiotic multistage syntheses', *Astrobiology*, 13(8), pp. 784–789.
634 doi: 10.1089/ast.2013.1057.

635 Shah, V. *et al.* (2019) 'Survival of RNA replicators is much easier in protocells than in surface-based, spatial systems', *Life*,
636 9(3). doi: 10.3390/life9030065.

637 Smith, J. M. and Szathmáry, E. (1995) *The Major Transitions in Evolution*. Oxford: Oxford University Press.

638 Solé, R. (2016) 'Synthetic transitions: Towards a new synthesis', *Philosophical Transactions of the Royal Society B:*
639 *Biological Sciences*, 371(1701). doi: 10.1098/rstb.2015.0438.

640 Stüeken, E. E. *et al.* (2013) 'Did life originate from a global chemical reactor?', *Geobiology*, 11(2), pp. 101–126. doi:
641 10.1111/gbi.12025.

642 Sutherland, J. D. (2017) 'Opinion: Studies on the origin of life-The end of the beginning', *Nature Reviews Chemistry*.
643 Macmillan Publishers Limited, 1, pp. 1–8. doi: 10.1038/s41570-016-0012.

644 Szabó, P. *et al.* (2002) 'In silico simulations reveal that replicators with limited dispersal evolve towards higher efficiency
645 and fidelity', *Nature*, 420(6913), pp. 340–343. doi: 10.1038/nature01187.

646 Szathmáry, E. (2005) 'In search of the simplest cell', *Nature*, 433(February), pp. 469–470.

647 Szathmáry, E. (2006) 'The origin of replicators and reproducers', *Philosophical Transactions of the Royal Society B:*
648 *Biological Sciences*, 361(1474), pp. 1761–1776. doi: 10.1098/rstb.2006.1912.

649 Szathmáry, E. (2015) 'Toward major evolutionary transitions theory 2.0', *Proceedings of the National Academy of Sciences*
650 *of the United States of America*, 112(33), pp. 10104–10111. doi: 10.1073/pnas.1421398112.

651 Szathmáry, E. and Demeter, L. (1987) 'Group selection of early replicators and the origin of life', *Journal of Theoretical*
652 *Biology*, 128(4), pp. 463–486. doi: 10.1016/S0022-5193(87)80191-1.

653 Takeuchi, N., Hogeweg, P. and Kaneko, K. (2017) 'Conceptualizing the origin of life in terms of evolution', *Philosophical*
654 *Transactions of the Royal Society A: Mathematical, Physical and Engineering Sciences*, 375(2109), pp. 1–10. doi:
655 10.1098/rsta.2016.0346.

656 Takeuchi, N., Poorthuis, P. H. and Hogeweg, P. (2005) 'Phenotypic error threshold; additivity and epistasis in RNA
657 evolution', *BMC Evolutionary Biology*, 5, pp. 1–9. doi: 10.1186/1471-2148-5-9.

658 Todisco, M. *et al.* (2018) 'Nonenzymatic Polymerization into Long Linear RNA Templated by Liquid Crystal Self-
659 Assembly', *ACS Nano*, 12(10), pp. 9750–9762. doi: 10.1021/acsnano.8b05821.

660 Trinks, H., Schröder, W. and Biebricher, C. K. (2005) 'Ice and the origin of life', *Origins of Life and Evolution of the*
661 *Biosphere*, 35(5), pp. 429–445. doi: 10.1007/s11084-005-5009-1.

662 Vasas, V. *et al.* (2012) 'Evolution before genes', *Biol. Direct*, 7(1), p. 1. doi: 10.1186/1745-6150-7-1.

663 Wachowius, F. and Holliger, P. (2019) 'Non-Enzymatic Assembly of a Minimized RNA Polymerase Ribozyme',
664 *ChemSystemsChem*, 1(1–2), pp. 12–15. doi: 10.1002/syst.201900004.

665 Woese, C. R. (2002) 'On the evolution of cells', *Proceedings of the National Academy of Sciences of the United States of*
666 *America*, 99(13), pp. 8742–8747. doi: 10.1073/pnas.132266999.

667 Woese, C. R. and Fox, G. E. (1977) 'The Concept of Cellular Evolution', *Journal of Molecular Evolution*, 10, pp. 1–6.

668 Wu, M. and Higgs, P. G. (2012) 'The origin of life is a spatially localized stochastic transition', *Biology Direct*. *Biology*
669 *Direct*, 7(1), p. 1. doi: 10.1186/1745-6150-7-42.

670 Yu, H., Zhang, S. and Chaput, J. C. (2012) 'Darwinian evolution of an alternative genetic system provides support for TNA
671 as an RNA progenitor', *Nature Chemistry*. Nature Publishing Group, 4(3), pp. 183–187. doi: 10.1038/nchem.1241.
672

673 Main figure titles and legends

674

675 **Figure 1. A sample of thresholds in origin of life research.** (a) Phase diagram representing necessary
676 conditions for a meteoritic impact to deliver a quantity of HCN above a threshold value of 10 mM (required for
677 its polymerization into nucleobases, assuming an oxidizing early Earth atmosphere). Diagram obtained by
678 mathematical modelling; meteorite radius represented on the x-axis; impact velocity on the y-axis; several
679 mixing depths below water surface are represented (from Parkos *et al.* (2018) with permission). (b) Diagram of
680 the photoactivated reactions from cis-DAMN to AICN compounds which are key intermediates in the prebiotic
681 synthesis of purine nucleotides. Ground and excited states respectively represented in solid and dotted lines;
682 dashed arrows indicate backward reactions. This pathway reveals different free-energy barriers of at least 52
683 kcal/mol that can be overcome thanks to light energy (from Boulanger *et al.* (2013) with permission). (c) Liquid-
684 crystal phase diagram delimiting 3 areas: a homogeneous phase of mixed RNA and polyethylene glycol (PEG)
685 (in blue), a liquid-liquid phase separation of RNA-rich droplets in PEG solution (in orange) and a liquid-liquid
686 crystals (LC) microdomains phase separation (in green). Going from one area to another is made possible by
687 varying temperature or molecular crowding (i.e. PEG concentration) (from Todisco *et al.* (2018) with
688 permission). (d) Graph describing an autocatalytic set of theoretical polymers that has reached catalytic closure

689 (threshold). The reactions are represented by nodes connecting reactants and products of ligation and cleavage
690 reactions. Dashed lines indicate catalysis and point from catalyst to catalyzed reaction (from Farmer et al.
691 (1986) with permission). (e) Phase diagram for an RNA polymerization model as a function of catalyst feedback
692 efficiency k and spontaneous polymerization rate r_0 . So called “dead” state characterized by slow spontaneous
693 rate of RNA synthesis, “living” state by rapid autocatalytic rate of RNA synthesis (from Wu and Higgs (2012)
694 with permission). (f) Diagram representing the conjectured transition from a state of progenote cells (genetic
695 transfer mainly achieved horizontally) to a state of speciated individuals (lineages resulting from vertical genetic
696 transfer). Passed the Darwinian Threshold, individuals go from a communal evolution to a Darwinian evolution.
697 Such a transition can be triggered by a decreased in competence initiated by environmental parameters or
698 selected mutations (from Goldenfeld, Biancalani and Jafarpour (2017) with permission).

699 **Figure 2. Phase diagrams for the replicase scenario.** (a) Phase diagram showing the areas where the replicase
700 regime is possible (green area delimited by the red and blue curves) in the parameter space (e , l), where e is the
701 error rate of the replicase and l the length of the copied sequences, including the replicase itself. The red curve
702 represents the function e_{max} that sets the maximal replicase error rate e_{max} for each given length l of the copied
703 sequence, and for a given selective advantage (s in equation (1)); it gives the maximal length of copied
704 sequences, for each given error rate e . When e is low enough, $e_{max}(l) \sim \frac{1}{l}$; when e is close to 1, equation (1) is
705 no longer valid and l exponentially tends towards 0 (Eigen, 1971). Above the red curve, the copied sequences
706 vanish in the error catastrophe. The blue curve represents the function e_{min} that sets the minimal error rate e_{min}
707 a replicase can reach due to biochemical considerations. As first approximation, higher fidelity needs to be
708 encoded in longer sequences. When e tends towards 1, the blue curve reaches a plateau corresponding to the
709 minimum length that a replicase must have to catalyze a phosphodiester bond between two nucleotides. For a
710 given length, there is no existing replicase under e_{min} . Note that l stands for the length of any copied sequence
711 in the case of the red curve, whereas it only stands for the length of the replicase in the case of the blue curve;
712 the representation of the two lengths on the same graph is possible thanks to the fact that the replicase regime
713 assumes that the replicase is itself subjected to replication as well. The blue and red curves are obtained by
714 merging models and experiments; their shape can therefore change. For example, in (b), the existence zone is
715 wider than in (a). In (c), there is no existence zone at all; as a consequence, the replicase scenario must be
716 revised or abandoned in this case. Figure (d) represents the distribution f , i.e. the number of available replicases
717 as a function of their copying error rate (at a given illustrative length of 200 nucleotides, as in (b)). The purple
718 zone bounded between e_{min} and e_{max} depicts the total number of possible sustainable replicases.

719 **Figure 3. Different ways of crossing thresholds.** The y-axis represents a relevant environmental variable
720 whereas the x-axis represents a variable of the system itself, in (a), (b) and (c). The phase diagrams are divided
721 in two: a green region β where the system displays a specific property p and a region α where it does not. (a) The
722 system, initially in point A, acquires the property p in point B thanks to an environmental change from E_1 to E_2 ,
723 i.e. via an extrinsic transition. Vesicle formation from a micellar solution can be so described, where E would be
724 for instance the concentration of dissolved CO_2 (Bachmann, Luigi and Lang, 1992). (b) The system undergoes a
725 transition from A to B because of an internal variation of the system, in a given environment, i.e. via an intrinsic
726 transition. Stochastic transitions from random polymerization to replicating polymers fit in this representation,
727 where X could describe the diversity of generated polymers (Mathis, Bhattacharya and Walker, 2017). (c) The
728 system acquires p (from A to B) thanks to an environmental change. It keeps this property in B” while the
729 environmental variable goes back to its initial value E_1 . This is made possible thanks to a transitory change of a
730 variable of the system itself in environment E_2 (from B to B’). For instance, the property p could be the ability to
731 sustain an autocatalytic network, the transient environmental change the shift between dry and rainy periods,
732 and the transition from B to B’ the accumulation of autocatalysts. The y-variable would then be environmental
733 hygrometry and the x-variable catalyst concentration. (d) Here, two independent systems in A and B fuse into a
734 single one in C that displays p , in environment E_1 . This is the case when autocatalytic networks get encapsulated
735 in compartments, endowing the novel system with the property to evolve through natural selection (Vasas *et al.*,
736 2012).

737 **Figure 4. Articulating different thresholds.** Figures (a), (b) and (c) represent combinations of two phase-
738 diagrams, with x- and y-axes describing relevant systemic and environmental variables (the representation is
739 simplified to fit a 2D illustration). The green region β and the blue region γ represent two regions where
740 properties p_β and p_γ can be acquired respectively. The arrows show different ways to cross a succession of two
741 thresholds. (a) **Entrenchment.** Region γ is included into region β so that the system must acquire p_β before
742 acquiring p_γ . In this configuration, p_β could stand for the ability to generate random polymers and p_γ for the
743 property of having an autocatalytic set of polymers (Mathis, Bhattacharya and Walker, 2017). (b) **Contingency**
744 **and transience.** Region γ partially intercepts region β so that the system can combine p_β and p_γ in C by first
745 acquiring either one of the two properties. Here p_β and p_γ could stand for the ability to generate one type of

746 genetic polymer or the other. The system in C would therefore generate both types of polymers at the same time,
 747 such as RNA and TNA. Transition from C to D, through a second threshold, shows that a specific property can
 748 be lost across phase transitions. It could be the loss of TNA that is not present in the actual living world
 749 (Cleaves *et al.*, 2019). **(c) Facilitation.** Getting p_{β} first lowers the threshold delineating p_{γ} . This is the case when
 750 compartmentalization (p_{β}) raises the error-threshold of a replicating system (p_{γ}) making it more likely to appear
 751 (Matsumura *et al.*, 2016). **(d)** This **Venn diagram** shows different ways of crossing a series of thresholds.
 752 Colored edges represent thresholds that delimit domains with novel properties. Each domain is denoted with a
 753 Greek letter. Points denoted with a capital Latin letter stand for a given system state. Arrows between points
 754 represent possible trajectories of a prebiotic system across successive domains. The figure exhibits contingency
 755 (the system can reach C or D from B), enabling constraint (the system in D can reach F but not E), accumulation
 756 (the system in C has accumulated properties gained in A and B), entrenchment (the property acquired in B
 757 remains in all other locations) and transience (the system in F has lost the property acquired in A). **(e)** This
 758 graph illustrates how crossing successions of thresholds may account for an increase in liveness over time.

759 **Figure 5. Threshold transitions in origin of life research.** Identifying a threshold in an origin of life scenario
 760 allows the formalization of a parameterized theoretical model. This model can be refined by the output of
 761 appropriate experiments, which reciprocally benefit from a refinement of the theoretical model. These back-and-
 762 forth relations make it possible to refine the threshold model. The parameters of the threshold model help to
 763 integrate several disciplines among which physics, chemistry or molecular biology. If the threshold is such that
 764 the transition from one state to another is possible, it can be used as a basis for modelling such a transition
 765 within a broader scenario for the transition from non-living to living matter. Transition possibilities are then
 766 constrained by hypothesized environments as determined by Earth sciences, geochemistry, astronomy etc.
 767 Plausibility estimates of such transitions allow one to build and estimate multi-stage scenarios articulated around
 768 well-identified thresholds. If a scenario reaches a dead-end, it needs to be revised and novel thresholds
 769 identified.
 770

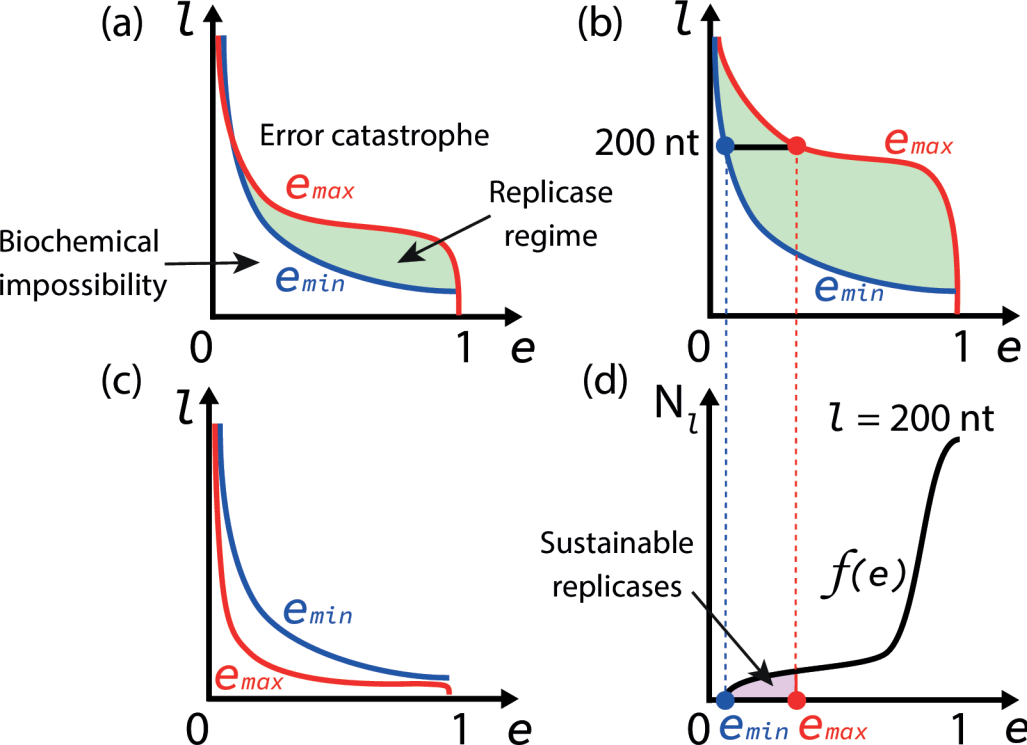
771 Main tables and legends

772

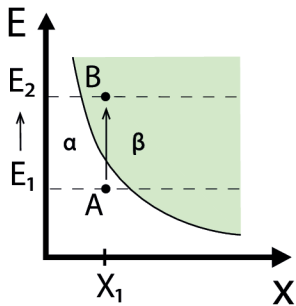
Threshold examples	System state before threshold	System state after threshold	Variables triggering the transition (in model or experiment)	Naturalized variables posited to have triggered the transition in an origin of life scenario
Chirality symmetry breaking (Budin and Szostak, 2010; Hawbaker and Blackmond, 2019)	Racemic state of a solution	Homochiral state of a solution	Enantiomeric excess	Presence of circularly polarized light, stereospecific crystallization, isotopic enantioselective initiators, auto-catalysis
Spontaneous polymerization (Monnard, Kanavarioti and Deamer, 2003; Baaske <i>et al.</i> , 2007; Lambert, 2008)	Solution of monomers	Solution of polymers	Concentrations of monomers, chemical activation	Ponds evaporation, freeze-thaw cycle, mineral surfaces, thermophoresis in hydrothermal vents, in situ closure in vesicles
Self-assembly of compartments (Bachmann, Luigi and Lang, 1992; Todisco <i>et al.</i> , 2018)	Solution of free constituents	Solution of molecular self-assembled compartments	Concentration of the constituents, salinity, pH, temperature, molecular crowding	Increase of CO ₂ concentration, day-night temperature variations, wet-dry cycles

Catalytic closure threshold (Kauffman, 1986)	Solution of polymers with few catalysts	Closed collective autocatalytic sets	Number of catalysts and reactions catalyzed	Spontaneous and effective synthesis of diverse polymers
Error threshold (Eigen, 1971; Takeuchi, Hogeweg and Kaneko, 2017)	Unreplicated polymers	Polymers copied by template-based replication	Selective advantage, copying error rate, polymers length	Selection of compartments, genotype-phenotype redundancy, mineral surfaces
Decay threshold (King, 1977; Szathmary, 2006; Vasas <i>et al.</i> , 2012)	No autocatalysis	Autocatalytic set	Kinetics, network topology, feedstock concentration	Transient depletion in reactants or rare product of pre-existing reactions
Darwinian threshold (Woese, 2002; Goldenfeld, Biancalani and Jafarpour, 2017)	Progenotes with high Horizontal Gene Transfer (HGT)	Speciated individuals with high Vertical Gene Transfer	HGT strength (i.e. competence), fitness	Decrease in cell density, nutrient limitation, alkaline shift, toxic chemicals release

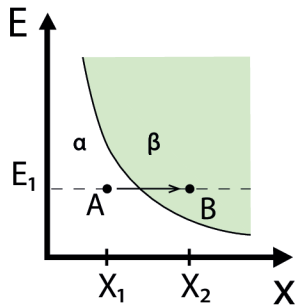
773 **Table 1. Examples of thresholds in origin of life scenarios.** Systems states before and after crossing the
774 threshold are listed, along with corresponding physico-chemical variables and prebiotically relevant phenomena.
775



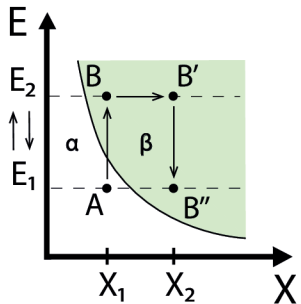
(a) Extrinsic transition



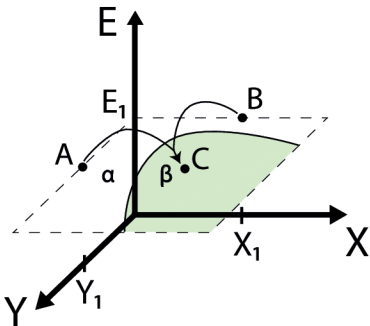
(b) Intrinsic transition



(c) Scaffolding transition



(d) Symbiotic transition



Origin of life scenarios

Prebiotic context

Threshold identification

Threshold articulation

Theory

Threshold crossing model (transition)

Experiment

Environmental model

formalizes

if scenario revision

assesses plausibility

if feasible

constrains

refines model

Physics, chemistry
molecular biology
etc.

Earth sciences,
geochemistry,
astronom etc.

Thresholds

